2014 IEEE International Conference on Robotics & Automation (ICRA)
Hong Kong Convention and Exhibition Center
May 31 - June 7, 2014. Hong Kong, China

Three Dimensional Trajectory Planner for Real Time Leader Following

Pedro Pereira, David Cabecinhas, Rita Cunha, Carlos Silvestre and Paulo Oliveira

Abstract— **This paper presents an on-line three dimensional trajectory planner for an unmanned vehicle following a Leader vehicle, where the Follower remains at a specified relative position with respect to the Leader. The planner defines the trajectory for a *virtual* vehicle that will be used as reference for the *real* Follower vehicle. The *virtual* Follower behaves like a three dimensional trailer attached to the Leader and its reference frame is used to specify the relative position vector. At the kinematic level, the proposed planner requires only the knowledge of the Leader's linear speed, but not its angular speed, and the Follower's trajectory can be generated on-line, in the sense that no *a priori* knowledge of the Leader's trajectory is required. Experimental results obtained with quadrotor vehicles are presented, which demonstrate the richness of the planned trajectories.**

I. Introduction

Multi-robot systems are an active research topic as they allow improved performance on accomplishing automated tasks. Multi-robot systems outperform single robot systems in situations where a wide area needs to be covered like terrain mapping or exploration of a sea floor [1], [2]. Another use case is load transportation where a formation of vehicles can handle loads that would be otherwise impossible for a single vehicle to transport [3]. Multiple vehicle formations are also employed in critical missions, where the objective is of paramount importance and robustness to vehicle loss is required [4].

In the Leader-Follower approach to formation control, the objective is for a Follower vehicle to remain at a fixed relative position, in a given reference frame, w.r.t. the Leader vehicle. The problem is completely characterized by the relative position vector and the reference frame where it is defined. The choice of reference frame plays an important role in the definition of the Follower's trajectory and in the sensory information necessary for computing such trajectory. A straightforward approach to the Leader-Follower formation definition is to specify the relative position vector in the inertial reference frame as in [5], [6]. This method results in a simple trajectory for the Follower, in the sense that both the Leader and the Follower describe an identical path, apart from a translation. This is inconvenient for mapping or terrain covering purposes because the Follower's path can overlap with the Leader's path, reducing the efficiency gains of using multiple aircraft.

Defining the relative position vector in a reference frame rotating with the Leader, such as the Leader's Serret-Frenet frame, results in Follower trajectories with more complex behavior. This approach has been proposed by several authors [7], [8], [9] but requires, at the kinematic level, the explicit knowledge of parameters that are not easily measured or estimated by the Follower, such as the Leader's reference frame angular velocity. Additionally, the works deal with a two dimensional setting and an extension for a three dimensional environment is not trivial, as it can lead to discontinuities or trajectories that are ill-defined as a consequence of choosing a Serret-Frenet reference frame.

A two part solution to the Leader-Follower formation problem in here proposed. First, a desired trajectory is computed for an ideal Follower vehicle, hereafter called *virtual* Follower. This reference trajectory is then used as a reference to a trajectory tracking controller that drives the real Follower vehicle to the desired trajectory. In this paper, we focus on the first problem of generating the follower trajectory and present experimental results for the complete planning/tracking problem using quadrotor vehicles. A new trajectory generation strategy is proposed to address the Leader-Follower problem where the relative position vector is specified in a reference frame attached to the *virtual* Follower, which is always well-defined. By imposing the appropriate kinematic constraints on the reference frame, the *virtual* Follower is made to behave as a three dimensional trailer attached to the Leader. The trajectory planner does not require, at the kinematic level, the knowledge of the Leader's path curvature and torsion but it still produces trajectories with a rich behavior that are not a simple translation of the Leader's path.

Quadrotors are aerial vehicles ideal for testing algorithms, due to their simplicity, high maneuverability, VTOL/hover capability and ability to track any trajectory within the limits of their actuation dynamics. Tracking controllers for quadrotor vehicles have been extensively studied in the literature, c.f. the survey article [10], and the *virtual* Follower trajectory generated by our planner can be used as reference for any generic tracking controller applied to the Follower vehicle.

The remainder of this paper is structured as follows. Section II presents the mathematical notation used throughout the paper. Section III describes the Leader-Follower problem. Section IV describes the trajectory planner equations and

This work was supported by project FCT PEst-OE/EEI/LA0009/2013 and by project FCT SCARVE (PTDC/EEA-CRO/102857/2008).

The work of P. Pereira was supported by a Research Student Grant under the FCT project PEst-OE/EEI/LA0009/2011.

The authors are with the Department of Electrical Engineering and Computer Science, and Institute for Robotics and Systems in Engineering and Science (LARSyS), Instituto Superior Técnico, Universidade Técnica de Lisboa, 1049-001 Lisboa, Portugal. D. Cabecinhas and C. Silvestre are also with the Department of Electrical and Computer Engineering, Faculty of Science and Technology of the University of Macau. {ppereira,dcabecinha}@isr.ist.utl.pt and {rita,cjs,pjcro}@isr.ist.utl.pt

proves the convergence of a Leader-Follower formation for a Leader describing a trimming trajectory. Section V describes the experimental set-up for the quadrotor vehicles and Section VI presents the obtained experimental results.

II. Notation

The configuration of a reference frame $\{B\}$ w.r.t. a frame $\{A\}$ is represented as an element of the Special Euclidean group, $({}^{A}_{B}\mathcal{R}, {}^{A}\mathbf{p}_{B}) \in \mathrm{SE}(3)$, where ${}^{A}\mathbf{p}_{B} \in \mathbb{R}^3$ is the position and ${}^{A}_{B}\mathcal{R} \in \mathrm{SO}(3)$ is the rotation matrix. For points in the inertial frame $\{\mathcal{I}\}$, the upper script frame letter is often omitted, i.e. $\mathbf{p}_B := {}^{\mathcal{I}}\mathbf{p}_B$. The following functions and symbols are used throughout this paper. The sign function $\mathrm{sgn}(x) : \mathbb{R} \mapsto \mathbb{R}$ satisfies $\mathrm{sgn}(0) = 0$ and $\mathrm{sgn}(x) = x|x|^{-1}$ for $x \neq 0$. The map $S(\mathbf{x}) : \mathbb{R}^3 \mapsto \mathbb{R}^{3\times 3}$ yields a cross-product skew-symmetric matrix such that $S(\mathbf{a})\mathbf{b} = \mathbf{a} \times \mathbf{b}$. The map $\Pi(\mathbf{x}) : \{\mathbf{x} \in \mathbb{R}^3 : \mathbf{x}^T\mathbf{x} = 1\} \mapsto \mathbb{R}^{3\times 3}$ where $\Pi(\mathbf{x}) = -S(\mathbf{x})^2$ yields a matrix that represents the orthogonal projection operator onto the subspace perpendicular to $\mathbf{x}$. The vectors $\mathbf{e}_i \in \mathbb{R}^3$ with $i = \{1, 2, 3\}$ are used to denote the unit vectors from the canonical basis for $\mathbb{R}^3$. We write as $f^{(i)}(t)$ the i^{th} time derivative of function $f(t)$ for $i = \{1, 2, \dots\}$.

III. Problem Statement

In a Leader-Follower problem, the *primary objective* is to keep the Leader and Follower vehicles separated by a fixed distance and a fixed direction specified in a given reference frame. We propose a two step approach to the problem which separates the problem of trajectory planning from that of trajectory tracking.

This paper focuses on the first step of generating the reference trajectory. The problem is addressed by considering a *virtual* vehicle that meets the *primary objective* at all times. The planner's output is then fed as a reference trajectory to the trajectory tracking controller implemented in the *real* Follower vehicle.

To describe the problem setup consider the inertial reference frame $\{\mathcal{I}\}$, the Leader's Frenet reference frame $\{\mathcal{L}\}$ defined by the pair $({}^{\mathcal{I}}_{\mathcal{L}}\mathcal{R}, \mathbf{p}_{\mathcal{L}}) \in \mathrm{SE}(3)$ and the *virtual* Follower reference frame $\{\mathcal{F}\}$ defined as $({}^{\mathcal{I}}_{\mathcal{F}}\mathcal{R}, \mathbf{p}_{\mathcal{F}}) \in \mathrm{SE}(3)$. The kinematics of ${}^{\mathcal{I}}_{\mathcal{L}}\mathcal{R}$ are given by ${}^{\mathcal{I}}_{\mathcal{L}}\dot{\mathcal{R}} = {}^{\mathcal{I}}_{\mathcal{L}}\mathcal{R}S(\boldsymbol{\omega}_{\mathcal{L}})$, with $\boldsymbol{\omega}_{\mathcal{L}}$ as the Leader's angular velocity, given by $\boldsymbol{\omega}_{\mathcal{L}} = \|\mathbf{v}_{\mathcal{L}}\| \begin{bmatrix}\tau_{\mathcal{L}} & 0 & \kappa_{\mathcal{L}}\end{bmatrix}^T$, and $\mathbf{v}_{\mathcal{L}}$, $\kappa_{\mathcal{L}}$ and $\tau_{\mathcal{L}}$ as the Leader's velocity, path curvature and path torsion, respectively.

In a Leader following strategy, the distance between Leader and *virtual* Follower is fixed and the relative position between them is given by the vector $\mathbf{d} = [\mathrm{d_x}\ \mathrm{d_y}\ \mathrm{d_z}]^T \in \mathbb{R}^3$ specified in the *virtual* Follower frame $\{\mathcal{F}\}$, i.e.

$$\mathbf{p}_{\mathcal{L}|\mathcal{F}} \equiv \mathbf{p}_{\mathcal{L}} - \mathbf{p}_{\mathcal{F}} = {}^{\mathcal{I}}_{\mathcal{F}}\mathcal{R}\mathbf{d}, \tag{1}$$

and the *primary* goal is to define the time evolution of ${}^{\mathcal{I}}_{\mathcal{F}}\mathcal{R}$.

IV. Trajectory Planner

To completely define the *virtual* Follower's trajectory, we act on the the kinematics of ${}^{\mathcal{I}}_{\mathcal{F}}\mathcal{R}$ which are given by ${}^{\mathcal{I}}_{\mathcal{F}}\dot{\mathcal{R}} = {}^{\mathcal{I}}_{\mathcal{F}}\mathcal{R}S(\boldsymbol{\omega}_{\mathcal{F}})$, where $\boldsymbol{\omega}_{\mathcal{F}} := [p_{\mathcal{F}}\ q_{\mathcal{F}}\ r_{\mathcal{F}}]^T \in \mathbb{R}^3$ is the angular velocity of the frame $\{\mathcal{F}\}$. The choice of $\boldsymbol{\omega}_{\mathcal{F}}$ has a significant impact on the planned trajectory. For example, if we trivially set $\boldsymbol{\omega}_{\mathcal{F}} = \mathbf{0}$ then the *virtual* Follower path would simply be a translation of the Leader's path. If we impose appropriate constraints on the angular velocity of the *virtual* Follower we can generate richer trajectories, e.g. by forcing the Follower vehicle to behave as a 3D trailer attached to the Leader. We now derive the conditions on the angular velocity $\boldsymbol{\omega}_{\mathcal{F}}$ and show that ${}^{\mathcal{L}}\mathbf{p}_{\mathcal{L}|\mathcal{F}}$ converges to a fixed vector, under some given assumptions.

A. Trajectory Planner for a Longitudinal Rigid Link

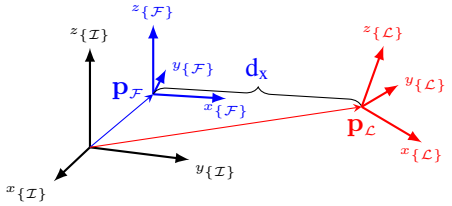

Fig. 1: Leader-Follower separated by a length $\mathrm{d_x}$ along the longitudinal axis of the *virtual* Follower reference frame

Consider a *virtual* Follower as a 3D trailer attached to a Leader by a longitudinal rigid link of length $\mathrm{d_x}$, as pictured in Figure 2, so that $\mathbf{d} = \mathrm{d_x}\mathbf{e}_1$. Let the 3D trailer body velocity be $\mathbf{u} := [u\ v\ w]^T$ so that $\dot{\mathbf{p}}_{\mathcal{F}} := {}^{\mathcal{I}}_{\mathcal{F}}\mathcal{R}\mathbf{u}$. Taking the time derivative of (1) it follows

$${}^{\mathcal{I}}_{\mathcal{F}}\mathcal{R}\begin{bmatrix}\mathbf{I} & S(-\mathbf{e}_1)\end{bmatrix}\begin{bmatrix}\mathbf{u} \\ \boldsymbol{\omega}_{\mathcal{F}}\mathrm{d_x}\end{bmatrix} = \mathbf{v}_{\mathcal{L}}. \tag{2}$$

In a three dimensional setting, a trailer is a vehicle that can only move longitudinally, i.e. $\mathbf{u} = u\mathbf{e}_1$, and it is allowed to yaw and pitch freely. Due to the nature of the longitudinal link, the roll rate $p_{\mathcal{F}}$ does not play any role in defining the position of the Follower and can be interpreted as a degree of freedom. Applying these restrictions to (2) it follows

$$u = \mathbf{e}_1^T\mathbf{u} = \mathbf{v}_{\mathcal{L}}^T\ {}^{\mathcal{I}}_{\mathcal{F}}\mathcal{R}\mathbf{e}_1, \tag{3}$$

$$\boldsymbol{\omega}_{\mathcal{F}} = \mathrm{d_x}^{-1}S(\mathbf{e}_1)\ {}^{\mathcal{F}}_{\mathcal{I}}\mathcal{R}\mathbf{v}_{\mathcal{L}} + p_{\mathcal{F}}\mathbf{e}_1. \tag{4}$$

For $p_{\mathcal{F}}(t) = 0$, the reference frame $({}^{\mathcal{I}}_{\mathcal{F}}\mathcal{R}, \mathbf{p}_{\mathcal{F}})$ is a parallel transport frame [11]. Notice that the trajectory generation is completely defined by (4), which only requires the knowledge of the Leader's linear speed and ${}^{\mathcal{I}}_{\mathcal{F}}\mathcal{R}$ (which is always well defined). The variables defined in what follows are only used for the purposes of analysis. We write the Leader's velocity as $\mathbf{v}_{\mathcal{L}} = \|\mathbf{v}_{\mathcal{L}}\|\ {}^{\mathcal{I}}_{\mathcal{L}}\mathcal{R}\mathbf{e}_1$ and introduce the shorthand notation

$$\mathcal{R} := \begin{bmatrix}\mathbf{r}_1 & \mathbf{r}_2 & \mathbf{r}_3\end{bmatrix} := {}^{\mathcal{L}}_{\mathcal{F}}\mathcal{R}.$$

For a longitudinal link connecting the two vehicles, the Leader-Follower formation is defined by the relative position vector ${}^{\mathcal{L}}\mathbf{p}_{\mathcal{L}|\mathcal{F}} = \mathbf{r}_1\mathrm{d_x}$ and, consequently, a rigid formation is obtained if $\mathbf{r}_1$ converges to a fixed vector. Rotations around $\mathbf{r}_1$ are allowed as they do not break the rigid formation. From (3), if the Leader is at rest so is the *virtual* Follower; in that case, the formation stays fixed w.r.t. $\{\mathcal{I}\}$. Hereafter, this trivial situation is ignored by assuming $\|\mathbf{v}_{\mathcal{L}}(t)\| \geq v_{\mathcal{L}}^{\min} > 0$

for all t.

1) Stability analysis of the three dimensional trailer formation for trimming trajectories : Consider a Leader vehicle describing a trimming trajectory characterized by constant torsion $\tau_{\mathcal{L}}$ and curvature $\kappa_{\mathcal{L}}$, i.e. a helix trajectory. The kinematics of the rotation matrix $\mathcal{R}$ are given by

$$\dot{\mathcal{R}} = S(\mathcal{R}\boldsymbol{\omega}_{\mathcal{F}} - \boldsymbol{\omega}_{\mathcal{L}})\mathcal{R}. \tag{5}$$

From the kinematics (5), it can be shown that $\mathbf{r}_1$ is a fixed vector if and only if the error $\mathbf{z}$ given by

$$\mathbf{z}(\mathbf{r}_1) = \Pi(\mathbf{r}_1)\left(\frac{\mathcal{R}\boldsymbol{\omega}_{\mathcal{F}}}{\|\mathbf{v}_{\mathcal{L}}\|} - \frac{\boldsymbol{\omega}_{\mathcal{L}}}{\|\mathbf{v}_{\mathcal{L}}\|}\right) \tag{6}$$

is zero. Notice that the error is defined to be velocity-independent, that is, it depends only on the characteristics of the Leader's path and not on the velocity with which it is described by the vehicle. Solving $\mathbf{z}(\mathbf{r}_1^\star) = \mathbf{0}$ and denoting the solution by its components $\mathbf{r}_1^\star = [\mathrm{r}_{11}^\star\ \mathrm{r}_{12}^\star\ \mathrm{r}_{13}^\star]^T$ we get

$$\mathrm{r}_{11}^\star = \pm\sqrt{\frac{\tilde{\mathrm{r}}_{11}^2}{2} + \sqrt{\mathrm{d_x}^2\tau_{\mathcal{L}}^2 + \left(\frac{\tilde{\mathrm{r}}_{11}^2}{2}\right)^2}}, \tag{7}$$

$$\mathrm{r}_{12}^\star = -\frac{1-\mathrm{r}_{11}^{\star 2}}{\kappa_{\mathcal{L}}\mathrm{d_x}},$$

$$\mathrm{r}_{13}^\star = \frac{1-\mathrm{r}_{11}^{\star 2}}{\mathrm{r}_{11}^\star}\frac{\tau_{\mathcal{L}}}{\kappa_{\mathcal{L}}}, \tag{8}$$

where $\tilde{\mathrm{r}}_{11}^2 = 1 - \mathrm{d_x}^2(\kappa_{\mathcal{L}}^2 + \tau_{\mathcal{L}}^2)$ and the additional relation

$$\begin{bmatrix}\tau_{\mathcal{L}} & 0 & \kappa_{\mathcal{L}}\end{bmatrix}\mathbf{r}_1^\star = \tau_{\mathcal{L}}\mathrm{r}_{11}^{\star -1}. \tag{9}$$

It can be shown the derivative of $\mathrm{r}_{11}^{\star 2}$ with respect to the variable $\gamma = (\tau_{\mathcal{L}}\mathrm{d_x})^2$ is always positive, which means that for a path with curvature $\kappa_{\mathcal{L}}$ we have

$$\lim_{\tau_{\mathcal{L}}\to 0}\mathrm{r}_{11}^{\star 2} \le \mathrm{r}_{11}^{\star 2} \le \lim_{\tau_{\mathcal{L}}\to\infty}\mathrm{r}_{11}^{\star 2} \Rightarrow 1-(\mathrm{d_x}\kappa_{\mathcal{L}})^2 \le \mathrm{r}_{11}^{\star 2} \le 1 \tag{10}$$

Equation (10) guarantees that (7)-(8) are well-defined and provide two solutions for $\mathbf{z}(\mathbf{r}_1^\star) = 0$ when $(\mathrm{d_x}\kappa_{\mathcal{L}})^2 < 1$. We now introduce Lemma 1 to help determine which of the two solutions coming from (7)-(8) is attained by the Leader-Follower formation, i.e. to which solution $\mathbf{r}_1$ converges to.

Lemma 1: Consider a Leader vehicle describing a path with non-zero velocity $\mathbf{v}_{\mathcal{L}}(t) \in \mathcal{C}^1(\mathbb{R}^3)$ and with curvature $\kappa_{\mathcal{L}}(t) \in \mathcal{C}^1$ and a *virtual* Follower vehicle imbued with kinematics (4). If the initial conditions for matrix $\mathcal{R} = {}^{\mathcal{L}}_{\mathcal{F}}\mathcal{R}$ verify $\mathrm{r}_{11}(0)\ \mathrm{sgn}(\mathrm{d_x}) \ge 0$ and if the Leader's path curvature is bounded such that $|\kappa_{\mathcal{L}}(t)\mathrm{d_x}|_\infty < 1$, then it follows that $\mathrm{r}_{11}(t)\ \mathrm{sgn}(\mathrm{d_x}) > 0$ for all $t > 0$.

Proof: Computing the time derivative of r_{11} yields

$$\dot{\mathrm{r}}_{11} = \|\mathbf{v}_{\mathcal{L}}\|\mathrm{d_x}^{-1}\left(1 - \mathrm{r}_{11}^2 + (\kappa_{\mathcal{L}}\mathrm{d_x})\mathrm{r}_{12}\right). \tag{11}$$

The function $\mathrm{r}_{11}(t) := \frac{\mathbf{v}_{\mathcal{L}}^T}{\|\mathbf{v}_{\mathcal{L}}\|}\ {}^{\mathcal{I}}_{\mathcal{F}}\mathcal{R}\mathbf{e}_1$ is continuous in time and consequently it cannot become negative without crossing $\mathrm{r}_{11} = 0$. However, for $\mathrm{r}_{11} = 0$ and $|\kappa_{\mathcal{L}}(t)\mathrm{d_x}|_\infty < 1$, it follows from (11) that $\dot{\mathrm{r}}_{11}\ \mathrm{sgn}(\mathrm{d_x}) > 0$ and $\mathrm{r}_{11}(t)\ \mathrm{sgn}(\mathrm{d_x})$ will increase and become positive. Then, if the initial condition $\mathrm{r}_{11}(0)\ \mathrm{sgn}(\mathrm{d_x})$ is positive or zero, it will remain positive for all subsequent time. ∎

We are now able to state the following Theorem, aggregating the results for the proposed Follower path generation and convergence of the Leader-Follower system to a rigid formation.

Theorem 2: Consider a Leader vehicle with non-zero velocity $\mathbf{v}_{\mathcal{L}}(t) \in \mathcal{C}^1(\mathbb{R}^3)$ describing a trimming trajectory path with constant curvature $\kappa_{\mathcal{L}}$ and torsion $\tau_{\mathcal{L}}$ and a *virtual* Follower imbued with kinematics (4). If the initial conditions for matrix $\mathcal{R} = {}^{\mathcal{L}}_{\mathcal{F}}\mathcal{R}$ verify $\mathrm{r}_{11}(0)\ \mathrm{sgn}(\mathrm{d_x}) \ge 0$ and if the Leader's path curvature is bounded such that $|\kappa_{\mathcal{L}}\mathrm{d_x}| < 1$, then the Leader and Follower vehicles converge to a rigid formation with relative position vector given by

$${}^{\mathcal{L}}\mathbf{p}^\star_{\mathcal{L}|\mathcal{F}} = \mathbf{r}_1^\star\mathrm{d_x},$$

with $\mathbf{r}_1^\star$ coming from the solution (7)-(8) that renders $\mathrm{r}_{11}^\star\ \mathrm{sgn}(\mathrm{d_x}) > 0$.

Proof: Consider the Lyapunov function $V(\mathbf{z}) = \frac{1}{2}\mathbf{z}^T\mathbf{z}$ with the error $\mathbf{z}$ defined as in (6). The time derivative of the error can be computed with the help of (5), yielding

$$\dot{\mathbf{z}} = -\|\mathbf{v}_{\mathcal{L}}\|\mathrm{d_x}^{-1}\mathrm{r}_{11}\mathbf{z} + \dot{\Pi}(\mathbf{r}_1)\left(\frac{\mathcal{R}\boldsymbol{\omega}_{\mathcal{F}}}{\|\mathbf{v}_{\mathcal{L}}\|} - \frac{\boldsymbol{\omega}_{\mathcal{L}}}{\|\mathbf{v}_{\mathcal{L}}\|}\right). \tag{12}$$

From (12), and noticing that $\dot{\Pi}(\mathbf{r}_1)\mathbf{z} = \mathbf{0}$, it follows that the time derivative of the Lyapunov function is

$$\dot{V}(t,\mathbf{z}) = -\mathrm{r}_{11}(t)\mathrm{d_x}^{-1}\|\mathbf{v}_{\mathcal{L}}\|\mathbf{z}^T\mathbf{z}. \tag{13}$$

From Lemma 1, and for the conditions stated in the Theorem, it follows trivially that the time derivative (13) is negative definite. The system dynamics for the error $\mathbf{z}$ has an exponentially stable point at the origin, resulting in convergence of $\mathbf{r}_1$ to the solution (7)-(8) with positive $\mathbf{r}_{11}^\star\mathrm{sgn}(\mathrm{d_x})$. ∎

From (13) it is clear that the solution in (7) satisfying $\mathrm{r}_{11}\mathrm{sgn}(\mathrm{d_x}) > 0$ is stable and the one satisfying $\mathrm{r}_{11}\mathrm{sgn}(\mathrm{d_x}) < 0$ is unstable. To gain some insight into the physical interpretation of this result, notice that the solution $\mathrm{r}_{11}\mathrm{sgn}(\mathrm{d_x}) > 0$ corresponds to a trailer being pulled (which is a stable operation) and the solution $\mathrm{r}_{11}\mathrm{sgn}(\mathrm{d_x}) < 0$ corresponds to a trailer being pushed (which is an unstable operation).

An interesting characteristic of the *virtual* Follower's equilibrium path is that it is also a curve of constant torsion, $\tau_{\mathcal{F}}$ and curvature $\kappa_{\mathcal{F}}$, with $\tau_{\mathcal{F}} = \frac{\tau_{\mathcal{L}}}{\mathrm{r}_{11}^{\star 2}}$ and $\kappa_{\mathcal{F}} = \frac{\sqrt{1-\mathrm{r}_{11}^{\star 2}}}{|\mathrm{d_x}|\mathrm{r}_{11}^\star}$.

B. Trajectory Planner for a Generic Rigid Link

We now consider a Leader-Follower formation with a generic relative position vector $\mathbf{d} \in \mathbb{R}^3$ where $\mathrm{d_y}$ and $\mathrm{d_z}$ are no longer constrained to be zero. In order for the path generation method to be an extension of the one described in Section IV-A we maintain the *virtual* Follower kinematics as defined in (4). Like with the longitudinal link situation, the choice of roll rate plays no role in the convergence of $\mathbf{r}_1$ and the reasoning in Theorem 2 is applicable, which guarantees convergence of $\mathbf{r}_1$ to $\mathbf{r}_1^\star$ remains valid. Unlike the previous situation, however, the roll rate does influence the generated path since we now have the components $\mathrm{d_y}$ and $\mathrm{d_z}$ that interact with $\mathbf{r}_2$ and $\mathbf{r}_3$ to generate the *virtual*

Follower's position.

For the purposes of studying the generated Follower path when the Leader is performing a trimming trajectory, the convergence of $\mathbf{r}_2$ and $\mathbf{r}_3$ is analyzed through the introduction of a new error

$$z_2 = \frac{p}{\|\mathbf{v}_{\mathcal{L}}\|} - \frac{\boldsymbol{\omega}_{\mathcal{L}}^T}{\|\mathbf{v}_{\mathcal{L}}\|}\mathbf{r}_1, \tag{14}$$

relating the angular velocities of the Leader and Follower along the direction $\mathbf{r}_1$. Keeping in mind that the Leader-Follower formation is defined by the relative position vector ${}^{\mathcal{L}}\mathbf{p}_{\mathcal{L}|\mathcal{F}} = \mathcal{R}\mathbf{d}$, a rigid formation is attained when the rotation matrix is constant. Given the rotation matrix kinematics (5) and convergence of the error (6) to zero, a rigid formation with a generic relative position vector is attained if and only if the error z_2 is zero.

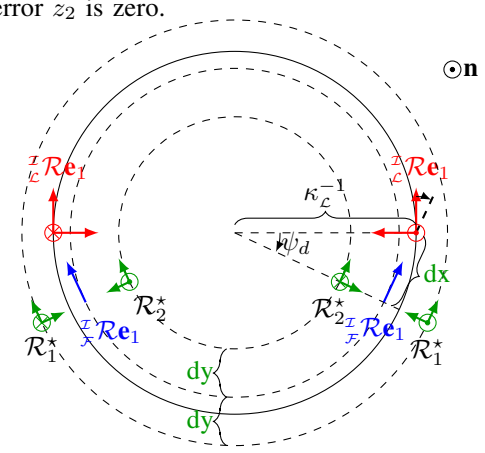

Fig. 2: Possible ${}^{\mathcal{L}}_{\mathcal{F}}\mathcal{R}$ configurations for $\mathrm{d_x}, \mathrm{d_y} > 0$

Similarly to what occurs for the error $\mathbf{z}$, there are two solutions that satisfy $z_2 = 0$. To have a better understanding of what the solutions correspond to, consider a Leader describing a circular path and $\mathbf{d} = [\mathrm{d_x}\ \mathrm{d_y}\ 0]$ with $\mathrm{d_x} > 0$ and $\mathrm{d_y} > 0$, as shown in Figure 2. In the figure, two Leaders are shown describing a path in clockwise and anti-clockwise directions. The notion of clockwise and anti-clockwise is arbitrary and it is defined in this work as follows: consider the unit vector $\mathbf{n}$, then if the Leader's angular velocity is *aligned* with $\mathbf{n}$, i.e. $\mathbf{n}^T\ {}^{\mathcal{I}}_{\mathcal{L}}\mathcal{R}\boldsymbol{\omega}_{\mathcal{L}} > 0$, the rotation is clockwise; if those are *misaligned*, i.e. $\mathbf{n}^T\ {}^{\mathcal{I}}_{\mathcal{L}}\mathcal{R}\boldsymbol{\omega}_{\mathcal{L}} < 0$, the rotation is anti-clockwise (an ambiguous situation exists if $\mathbf{n}^T\ {}^{\mathcal{I}}_{\mathcal{L}}\mathcal{R}\boldsymbol{\omega}_{\mathcal{L}} = 0$). For each of these situations, the Follower can meet the rigid formation specification $\mathbf{d}$ in two different ways, corresponding to the two solutions $\mathcal{R}^\star$ for $z_2(\mathcal{R}^\star) = 0$ as follows

$$\mathcal{R}_1^\star = \mathcal{R}_z(\psi_d) \quad \vee \quad \mathcal{R}_2^\star = \mathcal{R}_z(\psi_d)\mathcal{R}_x(\pi) \tag{15}$$

with where ψ_d is such that $\sin(\psi_d) = -\kappa_{\mathcal{L}}\mathrm{d_x}$ and $\mathcal{R}_x$ and $\mathcal{R}_z$ denote rotation matrices about the x and z axis, respectively.

We propose a trajectory planner that imbues the Follower vehicle with the following behavior. If the Leader's rotation is clockwise the Follower moves in an outer circle, corresponding to $\mathcal{R}_1^\star$ in (15). On the other hand, if the Leader's rotation is anti-clockwise the Follower moves in an inner circle, corresponding to the solution $\mathcal{R}_2^\star$ in (15). This behavior is proposed because the Leader's third axes ${}^{\mathcal{I}}_{\mathcal{L}}\mathcal{R}\mathbf{e}_3$ inverts direction from clockwise to anti-clockwise paths but it is desirable that the *virtual* Follower's third axes ${}^{\mathcal{I}}_{\mathcal{F}}\mathcal{R}\mathbf{e}_3$ remains *aligned* with $\mathbf{n}$, mimicking the behavior of a 2D trailer with $\mathrm{d_y} \neq 0$ [12]. For a Leader vehicle describing a planar path, the Follower is also required to describe a planar path in a plane parallel to that of the Leader, leading to $({}^{\mathcal{I}}_{\mathcal{L}}\mathcal{R}\mathbf{e}_3)^T\ {}^{\mathcal{I}}_{\mathcal{F}}\mathcal{R}\mathbf{e}_3 = \pm 1$. In that situation, the planes of motion where the vehicles evolve are separated by a distance $\mathrm{d_z}$, specified along the direction ${}^{\mathcal{I}}_{\mathcal{F}}\mathcal{R}\mathbf{e}_3$, and the condition $\mathbf{v}_{\mathcal{L}}^T\ {}^{\mathcal{I}}_{\mathcal{F}}\mathcal{R}\mathbf{e}_3 = 0$ is met. In order to remain in a planar path, the Follower vehicle cannot roll nor pitch. From (4) we have that $q \propto \mathbf{v}_{\mathcal{L}}^T\ {}^{\mathcal{I}}_{\mathcal{F}}\mathcal{R}\mathbf{e}_3$ and consequently, for the Follower to remain in a planar path the roll rate must satisfy $p \propto \mathbf{v}_{\mathcal{L}}^T\ {}^{\mathcal{I}}_{\mathcal{F}}\mathcal{R}\mathbf{e}_3$. With the previous comments in mind, the following roll rate is selected

$$\begin{aligned} p &= \mathrm{s}^\star(t)\mathbf{v}_{\mathcal{L}}^T\ {}^{\mathcal{I}}_{\mathcal{F}}\mathcal{R}\mathbf{e}_3|\mathrm{d_y}^{-1}| \\ &= \mathrm{s}^\star(t)\mathrm{r}_{31}\|\mathbf{v}_{\mathcal{L}}\||\mathrm{d_y}^{-1}| \end{aligned} \tag{16}$$

where $\mathrm{s}^\star(t) \in \mathcal{C}^2$ is an *altered* signum function that is obtained by solving the differential equation

$$\mathrm{s}^{\star(3)} + a_2\mathrm{s}^{\star(2)} + a_1\mathrm{s}^{\star(1)} + a_0\mathrm{s}^\star = a_0 \cdot \eta \tag{17}$$

where $\eta = \mathrm{sgn}(\mathbf{n}^T\ {}^{\mathcal{I}}_{\mathcal{F}}\mathcal{R}\mathbf{e}_3)\mathrm{sgn}(\mathbf{v}_{\mathcal{L}}^T\ {}^{\mathcal{I}}_{\mathcal{F}}\mathcal{R}\mathbf{e}_2)$ and a_0, a_1, and a_2 are such that $\{a_2 > 0, a_2a_1 > a_0\}$. The conditions on the coefficients of (17) ensure that $s^\star(t)$ converges asymptotically to the current value of η, which takes values in $\{-1, 0, 1\}$ and is allowed to change during the maneuver. The value of η is defined to ensure that the stable solution to $z_2(\mathcal{R}^\star) = 0$ follows the behavior specified in the preceding paragraph and thus mimics the motion of a 2D trailer for the case of planar trajectories. The function $\mathrm{s}^\star(t) \in \mathcal{C}^2$ is used instead of the discontinuous function η so as to provide a smooth enough reference position to the trajectory tracking controller. With the roll rate defined as in (16), the error z_2 in (14) can be rewritten as

$$z_2 = \mathrm{s}^\star(t)\mathrm{r}_{31}|\mathrm{d_y}^{-1}| - \begin{bmatrix}\tau_{\mathcal{L}} & 0 & \kappa_{\mathcal{L}}\end{bmatrix}\mathbf{r}_1.$$

Considering the equilibrium where (9) is satisfied and $s^\star(t) = \eta$, a solution $\mathcal{R}^\star$ can be computed for $z_2(\mathcal{R}^\star) = 0$. We provide the result for $\mathrm{r}_{33}^\star$ only,

$$\mathrm{r}_{33}^\star = \mathrm{sgn}(\mathrm{r}_{21}^\star)\frac{-\tau_{\mathcal{L}}^2|\mathrm{d_y}||\mathrm{d_x}| + \sqrt{\mathrm{r}_{11}^{\star 2}(1-\mathrm{r}_{11}^{\star 2}) - (\tau_{\mathcal{L}}\mathrm{d_y})^2}}{\kappa_{\mathcal{L}}|\mathrm{d_x}|\mathrm{r}_{11}^\star} \tag{18}$$

which is *uniquely* defined for $\kappa_{\mathcal{L}} \neq 0$ and exists provided that $\mathrm{d_y}$ is upper bounded by an expression, which is omitted due to space limitations. Qualitatively, an upper bound on $|\mathrm{d_x}|$ and $|\mathrm{d_y}|$ exist because beyond those bounds, the condition $\mathcal{R}\boldsymbol{\omega}_{\mathcal{F}} - \boldsymbol{\omega}_{\mathcal{L}} = 0$ cannot be met, in which case an equilibrium does not exist. (However, for planar paths $\mathrm{d_y}$ can take any value because $p_{\mathcal{F}} = 0$ regardless of $\mathrm{d_y}$). If $\kappa_{\mathcal{L}} = 0$, the Leader describes a rectilinear trajectory and there are no preferred directions for $\mathbf{r}_2^\star$ and $\mathbf{r}_3^\star$, leading to an infinitude of solutions

for $\mathcal{R}^\star$ (all solutions $\mathcal{R}^\star = \mathcal{R}_x(\phi)$, for all $\phi \in \mathbb{R}$, satisfy $z_2(\mathcal{R}^\star) = 0$).

To check the stability of the solutions consider the Lyapunov function $V_2(z_2) = \frac{1}{2}z_2^2$. The time derivative of the error z_2 is given by

$$\dot{z}_2(t, z_2) = -\eta\, \mathrm{r}_{21} \|\mathbf{v}_{\mathcal{L}}\| |\mathrm{d_y}^{-1}| z_2 + g(t) + h(t), \quad (19)$$

with $g(t) = \boldsymbol{\zeta}_{\mathbf{z}}^T \mathbf{z}$ and $h(t) = \boldsymbol{\zeta}_{\mathrm{s}^\star}^T \begin{bmatrix} \mathrm{s}^\star - \eta & \mathrm{s}^{\star(1)} & \mathrm{s}^{\star(2)} \end{bmatrix}$ and where $\boldsymbol{\zeta}_{\mathbf{z}}$ and $\boldsymbol{\zeta}_{\mathrm{s}^\star}$ are bounded. Then, under the conditions of Theorem 2 the term $g(t)$ converges exponentially fast to 0. Additionally, η is constant if we are sufficiently close to the stable equilibrium, implying that $h(t)$, which aggregates the errors due to using $s^\star(t)$ instead of η, also converges exponentially fast to 0. The Lyapunov function time derivative yields

$$\begin{aligned} \dot{V}_2 &= -\eta\, \mathrm{r}_{21} \|\mathbf{v}_{\mathcal{L}}\| |\mathrm{d_y}^{-1}| z_2^2 + z_2(g(t) + h(t)) \\ &= -\mathrm{sgn}(\mathbf{n}^T\, {}^{\mathcal{I}}_{\mathcal{F}}\mathcal{R}\mathbf{e}_3) |\mathrm{r}_{21}| \|\mathbf{v}_{\mathcal{L}}\| |\mathrm{d_y}^{-1}| z_2^2 + z_2(g(t) + h(t)), \end{aligned}$$

meaning that the system (19) is locally input-to-state stable (ISS), with $g(t) + h(t)$ as input, if and only if $\mathrm{sgn}(\mathbf{n}^T\, {}^{\mathcal{I}}_{\mathcal{F}}\mathcal{R}\mathbf{e}_3) > 0$ (notice that, for $\kappa_{\mathcal{L}} \neq 0$ and $\tau_{\mathcal{L}} = 0$ we have $\mathrm{r}^\star_{21} \neq 0$). The ISS property guarantees that in a given domain, if $g(t) + h(t)$ converges to zero, then z_2 will also converge to zero. Notice that the solution for which the *virtual* Follower third axis is aligned with $\mathbf{n}$, i.e. $\mathrm{sgn}(\mathbf{n}^T\, {}^{\mathcal{I}}_{\mathcal{F}}\mathcal{R}\mathbf{e}_3) > 0$, is stable, whereas the other solution with $\mathrm{sgn}(\mathbf{n}^T\, {}^{\mathcal{I}}_{\mathcal{F}}\mathcal{R}\mathbf{e}_3) < 0$ is unstable.

C. Trajectory Planner Summary

The proposed trajectory planner is a dynamic one, in the sense that it computes the *virtual* Follower's trajectory based on (1). The *virtual* Follower rotation matrix ${}^{\mathcal{I}}_{\mathcal{F}}\mathcal{R}$ can be interpreted as the *state* of the planner and whose kinematics are ruled by (4) and (16).

For the initialization, two options are available. If the Leader is initially at rest then the desired Follower position should be that which is closest to the *real* Follower. If the Leader is initially moving then the best guess is that it is moving straight, in which case the *virtual* Follower is initialized to match the equilibrium solution, i.e. ${}^{\mathcal{I}}_{\mathcal{F}}\mathcal{R}(0)\mathbf{e}_1 = \frac{\mathbf{v}_{\mathcal{L}}(0)}{\|\mathbf{v}_{\mathcal{L}}(0)\|}\mathrm{sgn}(\mathrm{d_x})$.

V. Experimental Set-up

The proposed trajectory planner was tested with two radio controlled Blade mQX quadrotor vehicles [13]. A VICON Bonita motion capture system [14], composed of 12 cameras and markers attached to the quadrotors, provides highly accurate position and orientation measurements for the Leader and Follower at a rate of 100Hz. The trajectory planner is implemented in a Matlab/Simulink model, which computes the Follower's position reference and feeds it to the quadrotors' trajectory tracker controller developed in [15] which requires a time-parametrized position reference of class $\mathcal{C}^3$. Consequently, the trajectory planner requires the knowledge of $\mathbf{p}_{\mathcal{L}}^{(i)}(t)$ for $i \in \{1, 2, 3\}$, which are obtained from the raw position measurements by means of dynamic differentiators.

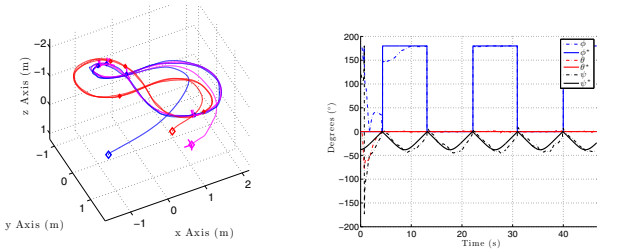

(a) Vehicle's trajectories (b) Euler Angles for $\mathcal{R}$ and for $\mathcal{R}^\star$

Fig. 3: Leader describing lemniscate path

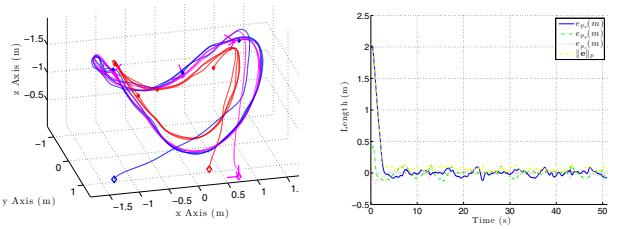

(a) Vehicle's trajectories (b) Tracking position error between *virtual* and *real* Follower

Fig. 4: Circular path with sinusoidal altitude variation

VI. Experiments

Three experiments are presented, where the Leader's path is depicted in red, the real Follower's path in blue and the *virtual* Follower's path in magenta, with the magenta reference frame being that of the *virtual* Follower, i.e. ${}^{\mathcal{I}}_{\mathcal{F}}\mathcal{R}$. In Figures 5(a), 5(b), 5(c), 3(a) and 4(a) the vehicles' positions are shown five times, with $\diamondsuit$ symbol for the initial position and $\bullet$ symbol for the other positions, equally spaced in time (elapsed time divided by four). In all experiments, the Leader's velocity was set at 0.5m/s and $\mathbf{n}$ was set to $-\mathbf{e}_3$. The position tracking error between the *virtual* Follower and the *real* Follower is only presented for one of the experiments in Figure 4(b).

Consider the xyz Euler angles for attitude parametrization, defined such that $\mathcal{R} := \mathcal{R}_z(\psi)\mathcal{R}_y(\theta)\mathcal{R}_x(\phi)$ and $\mathcal{R}^\star := \mathcal{R}_z(\psi^\star)\mathcal{R}_y(\theta^\star)\mathcal{R}_x(\phi^\star)$. We have shown that if the Leader describes a trimming path, i.e. a helix, the relative position between Leader and Follower converges to ${}^{\mathcal{L}}\mathbf{p}^\star_{\mathcal{F}|\mathcal{L}} = \mathcal{R}^\star\mathbf{d}$, where $\mathcal{R}^\star := \mathcal{R}^\star(\kappa_{\mathcal{L}}, \tau_{\mathcal{L}})$, with constant $\kappa_{\mathcal{L}}$ and $\tau_{\mathcal{L}}$. For non trimming paths, the matrix $\mathcal{R}$ is expected to *follow* the matrix $\mathcal{R}^\star := \mathcal{R}^\star(\kappa_{\mathcal{L}}(t), \tau_{\mathcal{L}}(t))$ where $\kappa_{\mathcal{L}}(t)$ and $\tau_{\mathcal{L}}(t)$ are time-varying. The Euler angles $\{\phi, \theta, \psi\}$ and $\{\phi^\star, \theta^\star, \psi^\star\}$ are presented in dashed and full lines, respectively in Figures 5(d) and 3(b), with $\{\phi^\star, \theta^\star, \psi^\star\}$ computed from (7)-(8) and (18) and $\{\phi, \theta, \psi\}$ computed from $\mathcal{R} := {}^{\mathcal{L}}_{\mathcal{I}}\mathcal{R}\, {}^{\mathcal{I}}_{\mathcal{F}}\mathcal{R}$.

Figures 5(a)-5(c) depict the paths for $\mathbf{d} = [0.4 \;\; -0.4 \;\; 0]^T$(m) and with the Leader quadrotor describing a path composed of two circular paths: one in a horizontal plane and the other in a plane tilted 45°, meaning that $\tau_{\mathcal{L}} = 0$ for most of the path, except during transition between planes. Notice the convergence of the *virtual* Follower's path to

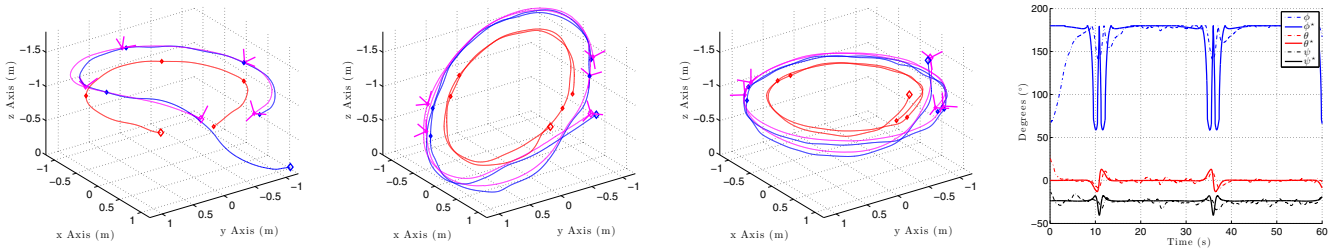

(a) Trajectories from $0s$ to $11s$ (b) Trajectories from $11s$ to $35s$ (c) Trajectories from $35s$ to $61s$ (d) Euler Angles for $\mathcal{R}$ and for $\mathcal{R}^\star$

Fig. 5: Leader describing circular paths in planes tilted $0°$ and $45°$

a zero-torsion path in the Leader's plane, which follows from $\mathrm{d}_z = 0$. Except during the transition between planes, the Leader describes trimming paths and for that reason $\{\phi, \theta, \psi\}$ converge to $\{\phi^\star, \theta^\star, \psi^\star\}$ which are constant (see Figure 5(d)). The *virtual* Follower's third axis ${}^{\mathcal{I}}_{\mathcal{F}}\mathcal{R}\mathbf{e}_3$ remains aligned with $\mathbf{n}$, i.e. $\mathrm{sgn}(\mathbf{n}^T\ {}^{\mathcal{I}}_{\mathcal{F}}\mathcal{R}\mathbf{e}_3) > 0$ ($\phi^\star = 180°$ because $\mathrm{sgn}(\mathbf{n}^T\ {}^{\mathcal{I}}_{\mathcal{L}}\mathcal{R}\mathbf{e}_3) < 0$).

In Figure 3(a), $\mathbf{d} = [0.35\ 0.35\ -0.3]^T$(m) and the Leader quadrotor describes a lemniscate path in a horizontal plane, defined as

$$\mathbf{p}(\gamma) = 1.7\,\mathcal{R}_z\left(-\frac{\pi}{4}\right)\left[\frac{\cos(\gamma)}{1+\sin^2(\gamma)} \quad \frac{1}{2}\frac{\sin(2\gamma)}{1+\sin^2(\gamma)} \quad -1.1\right]^T \text{(m)}$$

with $\dot{\gamma} = \frac{0.5}{1.7}\sqrt{1+\sin^2(\gamma)}$. Again, $\tau_{\mathcal{L}} = 0$ and the *virtual* Follower converges to a plane parallel to the Leader's plane, without any prior knowledge that the Leader is moving in that plane. The Leader's path is not a trimming one, consequently $\{\phi^\star, \theta^\star, \psi^\star\}$, presented in Figure 3(b), vary in time. Notice that ψ *follows* $\psi^\star$ with a certain delay; θ and $\theta^\star$ are zero because the trajectory is planar; and ϕ and $\phi^\star$ switch between $0°$ and $180°$ for clockwise and anticlockwise rotations, respectively. Because ${}^{\mathcal{I}}_{\mathcal{F}}\mathcal{R}\mathbf{e}_3$ is aligned with $\mathbf{n}$, the Follower's curvature is smaller when the Leader's rotation is clockwise and larger when the Leader's rotation is anticlockwise.

Finally, in Figure 4(a), $\mathbf{d} = [0.4\ 0.4\ 0]^T$(m) and a Leader quadrotor describes a circular path with a sinusoidal altitude variation. The Leader's path is not planar but the *virtual* Follower, which behaves like a *3D trailer* attached to the Leader, is at each moment compelled to remain in the osculating plane of the Leader (spanned by ${}^{\mathcal{I}}_{\mathcal{L}}\mathcal{R}\mathbf{e}_1$ and ${}^{\mathcal{I}}_{\mathcal{L}}\mathcal{R}\mathbf{e}_2$). As shown in Figure 4(b), the tracking error converges to zero, which is equivalent to the convergence of the magenta and blues lines.

VII. Conclusion

In this paper, a real-time three dimensional trajectory planner for Leader following is presented. The proposed solution maintains a fixed relative position vector between Leader and Follower, written in a *virtual* Follower reference frame, and it does not require *a priori* knowledge of the Leader's path. For a longitudinal relative position vector, the *virtual* Follower reference frame is that of a three dimensional trailer attached to the Leader. Convergence of the formation for a Leader describing a trimming trajectory was shown, considering both a longitudinal and a generic relative positive vector. Experiments performed with quadrotor vehicles were conducted that demonstrate the richness and suitability of the generated trajectories. Directions for future work include studying a sequence of n-trailers and incorporating a collision avoidance strategy.

References

[1] H. Yamaguchi. A distributed motion coordination strategy for multiple nonholonomic mobile robots in cooperative hunting operations. In *Proceedings of the 41st IEEE Conference on Decision and Control*, volume 3, pages 2984–2991 vol.3, 2002.

[2] James G. Bellingham and Kanna Rajan. Robotics in remote and hostile environments. *Science*, 318(5853):1098–1102, 2007.

[3] J. Fink, N. Michael, S. Kim, and V. Kumar. Planning and control for cooperative manipulation and transportation with aerial robots. *The International Journal of Robotics Research*, 30(3), March 2011.

[4] T.H. Summers, Changbin Yu, and B. D O Anderson. Robustness to agent loss in vehicle formations and sensor networks. In *47th IEEE Conference on Decision and Control*, pages 1193–1199, 2008.

[5] G. Wen, Z. Peng, Y. Yu, and A. Rahmani. Planning and control of three-dimensional multi-agent formations. *IMA Journal of Mathematical Control and Information*, 2012.

[6] S. Mastellone, D. M. Stipanovic, C. Graunke, K. Intlekofer, and M. Spong. Formation control and collision avoidance for multi-agent non-holonomic systems: Theory and experiments. *I. J. Robotic Res.*, 27(1):107–126, 2008.

[7] R. Cui, S. Sam Ge, B. How, and Y. Choo. Leader follower formation control of underactuated autonomous underwater vehicles. *Ocean Engineering*, Volume 37:1491–1502, December 2010.

[8] Zhaoxia Peng, Guoguang Wen, Ahmed Rahmani, and Yongguang Yu. Leader–follower formation control of nonholonomic mobile robots based on a bioinspired neurodynamic based approach. *Robotics and Autonomous Systems*, June 2013.

[9] G.L. Mariottini, F. Morbidi, D. Prattichizzo, G.J. Pappas, and K. Daniilidis. Leader-follower formations: Uncalibrated vision-based localization and control. In *2007 IEEE International Conference on Robotics and Automation*, pages 2403–2408, 2007.

[10] Minh-Duc Hua, T. Hamel, P. Morin, and C. Samson. Introduction to feedback control of underactuated VTOL vehicles: A review of basic control design ideas and principles. *Control Systems, IEEE*, 33(1):61–75, 2013.

[11] Andrew J. Hanson and Hui Ma. Parallel transport approach to curve framing. Technical report, 1995.

[12] V. Roldão, R. Cunha, D. Cabecinhas, P. Oliveira, and C. Silvestre. A novel leader-following strategy applied to formations of quadrotors. In *European Control Conference (ECC)*, 2013.

[13] "Quadrotor specifications". http://www.bladehelis.com, September 2013.

[14] "Vicon system". http://www.vicon.com, September 2013.

[15] D. Cabecinhas, R. Cunha, and C. Silvestre. Saturated output feedback control of a quadrotor aircraft. In *American Control Conference (ACC)*, pages 4667–4602, 2012.